Colloid Polym Sci 277:234–241 (1999)

ORIGINAL CONTRIBUTION

S.K. Danchinov
Y.D. Shibanov(†)
Y.K. Godovsky

The effect of glass transition on phase separation in binary off-critical blends: different coarsening regimes near the nonequilibrium percolation threshold

Accepted: 21 September 1998

S.K. Danchinov · Yu. D. Shibanov
Yu. K. Godovsky (✉)
Department of Polymer Materials
Karpov Institute of Physical Chemistry
ul. Vorontsovo pole 10
Moscow 103064, Russia
Fax: +7-095-9752450

Abstract The nonequilibrium percolation threshold was shown to take an intermediate position between binodal and mean-field spinodal. Below the nonequilibrium percolation threshold, a bicontinuous phase structure was produced. This percolation structure, depending on supersaturation, breaks down to ramified clusters slowly assuming a spherical droplet form or contracts to the center of the sample. In the latter case, at late stages, secondary phase separation is observed.

Key words Oligomers – Phase separation – Glass transition – Spinodal percolation – Nonequilibrium percolation threshold

Introduction

For experimental studies, polymer blends offer evident and substantial advantages because they are characterized by a slow mode of the phase separation. These advantages of polymer blends allowed identification of nucleation and growth of droplet phases in metastable regions [1] as well as spinodal decomposition in unstable regions [2–5]. Theoretical investigations showed that, for off-critical mixtures, spinodal decomposition should take place at lower supersaturations compared with those predicted from the classical spinodal [6]. The boundary between the two modes of phase separation is referred to as a nonequilibrium percolation threshold (NPT), which takes an intermediate position between the regime of growth of isolated droplets or clusters and the regime of the development of a nonequilibrium percolation structure, which is produced at early stages of phase separation and, at late stages, breaks down into droplets. However, the lack of experimental data concerning phase separation in the boundary region between the two regimes is quite evident.

The systems where the upper critical solution temperature is close to the glass transition temperature of one of the components involved in the polymer blend are more convenient for such an investigation for the following reason. Near the glass transition temperature, phase separation is affected by glass solidification in one of the two phases. Within this phase, viscosity should dramatically increase with time, and phase separation should be noticeably retarded. This retardation allows the detailed characterization of the evolution of the polymer morphology at temperatures near the NPT, which usually escapes identification in simple fluid systems.

We report our observations of a novel phase-separation phenomena in off-critical mixtures with a low volume fraction of the polymer phase (minority phase), whose glass transition temperature is close to the NPT. At supersaturations close to the NPT, spinodal decomposition is accompanied by a breakdown of the percolation network into individual ramified clusters, whereas at higher supersaturations far from the NPT no breakdown of the percolation structure is observed, and spinodal decomposition proceeds via the contraction of the percolation network to the center of the sample. In the latter case, at late stages of coarsening, the phase formed experiences a well-pronounced secondary phase separation.

Experimental section

We used mixtures of oligomers of styrene (PS) and butadiene (PB) [polystyrene (PS): $M_n = 1790$, $M_w/M_n < 1.06$; polybutadiene (PB): $M_n = 498$, $M_w/M_n = 1.16$]. Oligomer PS was from Knauer (Berlin), oligomer PB was from PSS (Polymer Standards Service, Mainz) and they were used as received.

In the case of the PS/PB mixtures, the corresponding phase diagram is characterized by an upper critical solution temperature T_c of 306.5 K (Fig. 1). The critical concentration was calculated using the following relationship:

$$\phi_c = 1 \Big/ \left[1 + (r_2 v_2 / r_1 v_1)^{1/2}\right] \ , \qquad (1)$$

where $r_1 = 9$ and $r_2 = 17$ stand for the degrees of polymerization of OB and OS, respectively; $v_1 = 99.63$ Å^3 and $v_2 = 178.04$ Å^3 are the corresponding molar volumes; the critical concentration was estimated to be 36.9 vol% of OS.

Cloud points were estimated from the sharp decrease in the intensity of transmitted light as detected by photodiodes. The values of the cloud temperature are controlled by the cooling rates, and with increasing cooling rate they level off (Fig. 2). At cooling rates in the range 2–5 K/min, the cloud point corresponds to the appearance of rippled structures or ramified clusters (without the formation of droplet morphology), which are able to produce strong light scattering (Fig. 3a). For polymer blends with different compositions, the values of the cloud temperature extrapolated to high cooling rates are presented in the phase diagram as a cloud-point curve (CPC).

The glass transition curve was estimated by differential scanning calorimetry. In our studies, we used a Perkin Elmer DSC-7, and the heating rate was 20 K/min. The glass transition curve intersects the right branch of the CPC at the *F*-point, the coordinates of which are 13 vol% PB and 288 K (in the two-phase region, only the high-temperature horizontal branch is presented in Fig. 1, and the low-temperature branch is not shown).

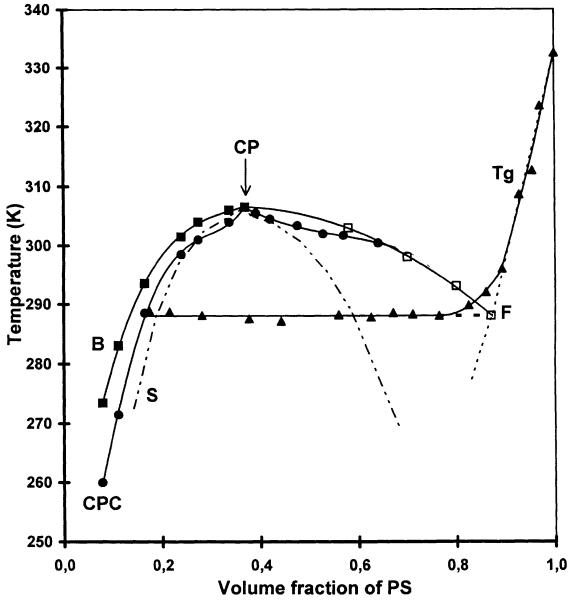

Fig. 1 Phase diagram for the polystyrene (*PS*) polybutadiene (*PB*) mixture at positive temperatures. *B* is the coexistence curve: the *left branch* is from the experimental points, and the *right branch* was calculated using Eq. (3); *CPC* is the cloud-point curve; *S* is the mean-field spinodal calculated from experimental values of the Flory interaction parameter; *CP* is the upper critical solution temperature; T_g is the glass transition curve; *F* is the point of intersection of the binodal and the glass transition curves

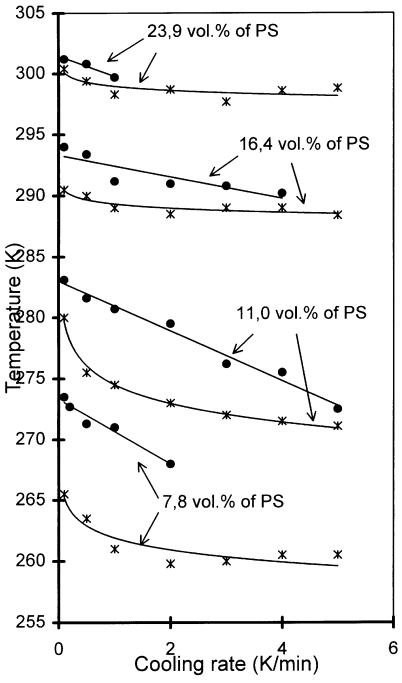

Fig. 2 Cloud-point temperature (*) and droplet-appearance-point temperature (●) as functions of the cooling rate in the PS/PB system

The left branch of the coexistence curve was obtained from direct observations of the appearance of droplets induced by cooling of homogeneous mixtures (Fig. 3b). The temperatures corresponding to the appearance of droplet morphology show a linear dependence on the cooling rate when cooling rates vary from 0.1 to 1 K/min. For mixtures with different composition, the corresponding coexistence curves were obtained by extrapolating the above dependences to zero cooling rate (Fig. 2).

The construction of the right branch of the binodal is a difficult experimental task because in this region polymer mixtures are characterized by high viscosity. Therefore, this portion of the coexistence curve was calculated from the left branch with the assumption that the generally accepted temperature dependence of the Flory interaction parameter holds:

$$\chi = a + b/T \ . \qquad (2)$$

In this relationship, fitting parameters $a = -0.61$ and $b = 258.4$ K were estimated from the critical temperature and composition of coexisting phases at the temperature corresponding to the *F*-point. The Flory interaction parameter was calculated from the Flory–Huggins relationship for the best-fit free-energy density [7]:

$$f(\phi) = \phi \ln \phi / r_2 + (1 - \phi) \ln(1 - \phi)/r_1 + \chi \phi (1 - \phi) \ . \qquad (3)$$

The mean-field spinodal was calculated according to the Flory–Huggins model from the values of the Flory interaction parameter estimated from the binodal:

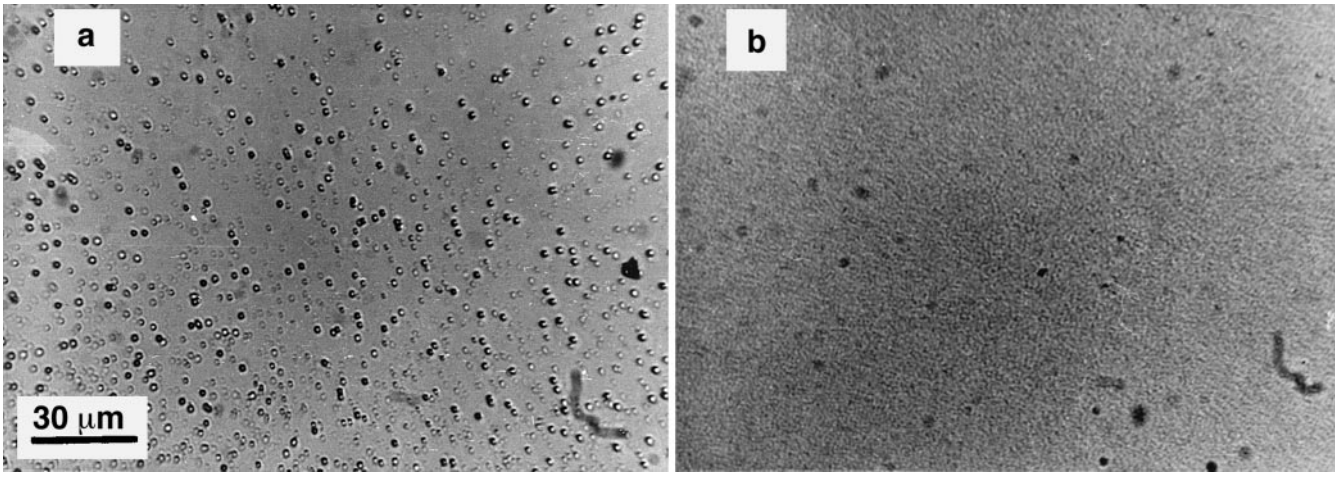

Fig. 3 Morphology of the PS/PB mixture (16.9 vol% PS) at the early stages of phase separation as a function of cooling rate: **a** 0.1 K/min; **b** 5.0 K/min The same scale is used for **a** and **b**

$$\chi_s(T) = (1/2)(1/r_1\phi_1 + r_2\phi_2) \quad . \tag{4}$$

The thickness of the test samples sandwiched between two glass sheets was 80–100 μm. Quenching of homogeneous samples was carried out by taking the samples from the thermal chamber and placing them onto a Mettler FP82 hot stage. The temperature was attained within 15 s, and this time is much lower than the time scales which were used in our studies to follow the development of polymer morphology (from several minutes to several weeks). Macroscopic flow was absent.

Results and discussion

Coupling of phase separation and glass transition can be geometrically described on a phase diagram as an intersection of the binodal and the glass transition curves (*F*-point on Fig. 1).

Excluding the vicinity of the critical point, the experimental value of the factor β involved in the scaling relationship

$$(\phi'' - \phi') \sim [(T_g - T)/T_g]^{\beta} \tag{5}$$

coincides with the mean-field approximation, despite the low molecular masses of the components. In the case of the mean-field theoretical description, it was found that there should be an intermediate regime of the phase separation between the regime of growth of isolated droplets or clusters and the regime of the development of a nonequilibrium percolation structure. Our experiments confirm this theoretical prediction. As evidenced by our direct morphological observations and from laser light-scattering experiments, the CPC is nothing else but the NPT. At PS concentrations below 25%, the CPC is located above the mean-field spinodal. This conclusion is based on the following experimental results.

The morphological changes are characterized at a temperature $T = 293$ K. In the two-phase region, the temperature interval of the glass transition was estimated from the width of the heat capacity peak and is equal to $\Delta T = 20$ K. Hence, the temperature of 293 K is slightly above the glass transition temperature but lies within the temperature interval of the glass transition.

In this viscous system, high cooling rates are associated with quenching through the metastable region. After quenching the homogeneous off-critical mixtures down to 293 K and at supersaturation beyond the NPT ($\phi_p \sim 18\%$ of PS), droplet morphology is produced. At supersaturation below the NPT, development of the percolation pattern takes place, and this pattern is similar to the bicontinuous structure produced by spinodal decomposition (Figs. 4a, 5a). In the case of laser light scattering, a diffraction ring is observed, which is also characteristic of spinodal decomposition. This evidence suggests that the bicontinuous spinodal structure may be produced below the NPT but beyond the classical spinodal (21% of PS at 293 K). Further evolution of this structure is controlled by its remoteness from the NPT. Near the NPT percolation structure breaks down with time into individual ramified clusters (dynamic percolation) (Fig. 4). Then, the ramified clusters tend to lower their free surface and assume a spherical shape. Far from the NPT, coarsening of the percolation structure is observed, and this process proceeds without any breakdown of the network morphology (static percolation) (Fig. 5). This coarsening is accompanied by a macroscopic contraction of the network toward the center of the samples, and this process manifests itself by the appearance of a cloudy region inside the transparent samples as evidenced by direct observations with the naked eye (Fig. 5e). This contraction of the percolation network without any disruption is observed at ϕ_s (293 K) about 21% of PS to

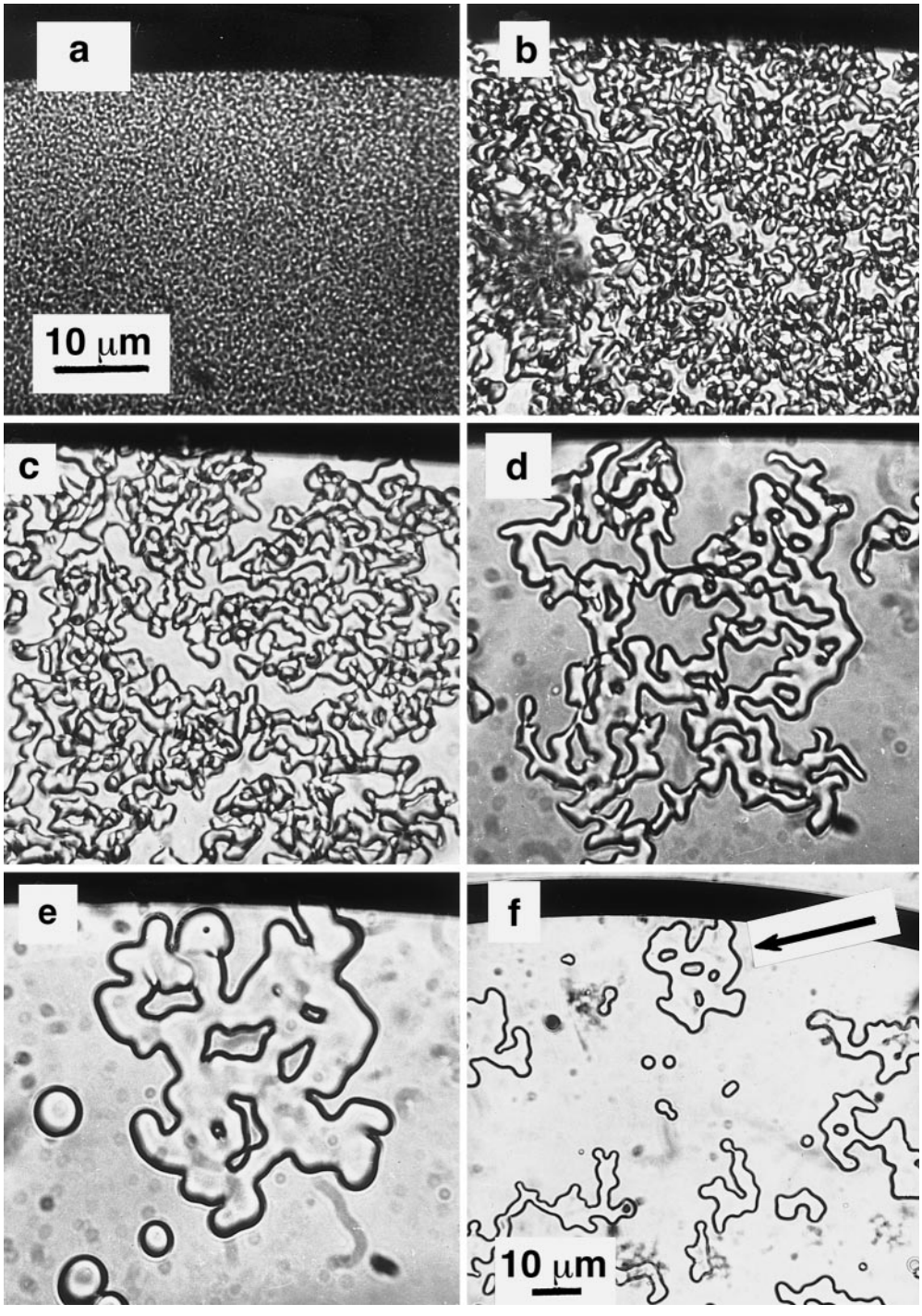

Fig. 4a–f Evolution of morphology during phase separation in binary mixture containing 18.5 vol% PS (between the nonequilibrium percolation threshold and the mean-field spinodal curves) at 293 K. **a** 4 min after quenching, **b** 164 h, **c** 362 h, **d** 748 h, **e** 1027 h, **f** 1364 h (the same cluster as in previous photo is shown by the *arrow*). The same scale is used for **a–e**

about ϕ_c. As far as we know, this mode of coarsening has been recognized for the first time. At late stages within the coarsening network, a secondary phase separation takes place and proceeds via the formation of droplets of the PB-enriched phase (Fig. 5d).

The stability of the percolation network to breakdown into clusters may be rationalized by the effect of the glass transition in the percolation phase. When the phase diagram shows the *F*-point, a traditional pattern of spinodal decomposition should be preserved [8, 9] but the following important correction should be introduced. In these systems, within the single-phase region, the isothermic viscosity $\eta(\phi)$ measured at temperatures between the glass transition temperatures of the com-

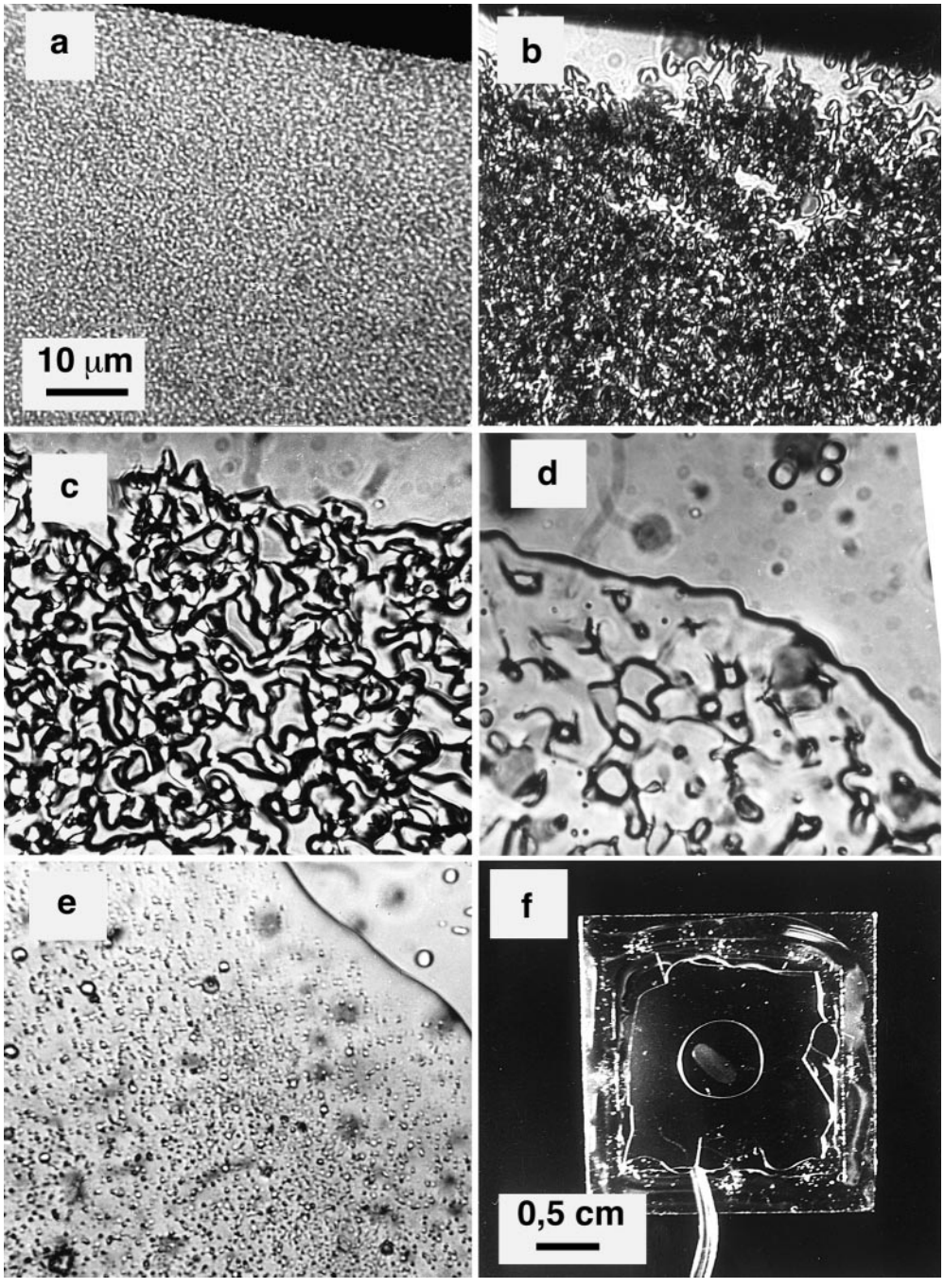

Fig. 5a–f Evolution of the percolation structure in binary mixtures containing 23.9 vol% PS at 293 K (below mean-field spinodal): **a** 2 min after quenching, **b** 96 h, **c** 844 h, **d** 1124 h, **e** 1464 h, **f** view of sample (macroscale). The same scale is used for **a–e**

ponents is controlled by the composition. This value changes by several orders of magnitude, from the values characteristic of melts to the values typical of the glassy state [10] (concentration glass transition). Concentration fluctuations, including those taking place during phase separation, are accompanied by strong fluctuations in viscosity and concomitant changes in diffusion coefficients, which become functions of the spatial coordinate and time. Coupling between concentration fluctuations and viscosity fluctuations as well as concomitant changes in diffusion coefficients and the shear modulus, which increases from zero at the glass transition region, are responsible for the specific features of the phase separation at temperatures near or below the glass transition temperature of one of the phases.

Two reasons related to the glass transition can be suggested to explain the stability of the percolation structure. The first reason is provided by the high ratio

λ_c/R (λ_c is the wavelength corresponding to the maximum capillary instability in the shape excitation spectra of an infinite cylinder, and R is the radius of the cylinder), which is controlled by the very high ratio between viscosities η'/η (η' and η stand for the viscosities within the matrix and the percolation phases, respectively) [11]. An alternative explanation is provided by the high rigidity of the percolation network (nonzero values of the shear modulus). At temperatures near the glass transition temperature T_g, the viscosity η' of the percolation phase is about 10^{12} Pa s [12], and the viscosity η of the fluid PB-enriched phase may be estimated as about 10^{-1} Pa s [13]. Hence, the ratio η'/η is about 10^{13}, and $\lambda_c > 10^3 R$. At $R = 10$ μm, λ_c exceeds 1 cm, i.e., this value is comparable to the sizes of the test samples. However, the main contribution to an improved stability of the percolation network is likely to be provided by the rigidity of the network: when the spinodal structure produced at 293 K is heated within the two-phase region by 5 K, its fast breakdown is observed. As a result of this heating, the viscosity changes by about 1 order of magnitude, and the values of λ_c are of a macroscopic scale. In this case, the shear modulus becomes almost zero.

The stability of the percolation network allows us to explain three observed phenomena

1. The NPT at a low volume fraction of the phase formed.

2. Contraction of the percolation structure to the center of the sample.

3. Secondary phase separation.

1. The position of the NPT ($\phi' < \phi_p < \phi_s$) appears to be in quantitative agreement with theoretical speculations. The values of the factor $\beta = 0.5$ allows one to conclude that in the off-critical PS/PB mixtures, far from the critical point, the mean-field regime of phase separation is observed. According to Binder [14], this regime involves a gradual transition from spinodal nucleation to spinodal decomposition, and the onset of this transition is observed at $\phi < \phi_s$. This conclusion is proved by our direct observations. There are several ways to determine the percolation process. Quenching of the percolation network by glass solidification at early stages of phase separation allows us to classify the NPT as dynamic spinodal [15, 16] and to attribute this NPT to the first appearance of the intermediate percolation. At the NPT, the value of the volume fraction of the minority phase is about 0.04, i.e., it is much lower than the 0.16 observed for equilibrium random percolation [17].

2. In the range between ϕ_p and ϕ_s, a slow breakdown of the percolation structure into clusters is also associated with improved stability of the percolation network. However, this stability is unable to provide the static percolation at the low volume fraction of the minority phase and, consequently, at low R. With increasing volume fraction of the minority phase, i.e., at $\phi > \phi_s$, the stability of the percolation structure increases, and its coarsening proceeds without any breakdown to clusters. In our experiments, ϕ_s is the approximate boundary associated with the transition from dynamic to static percolation, and the reasons responsible for this transition are still unclear: whether this transition is provided by an increase in the volume fraction of the new phase or by changes in the mode of phase separation.

3. Secondary phase separation, which takes place during coarsening, is likely to be related to a slow diffusion in the percolation phase. As a result, the concentration within this phase does not approach the equilibrium values because of a dramatic decrease in the diffusion rates at early stages of the spinodal decomposition. For a long period of time, this phase exists in the metastable region or unstable region in the corresponding phase diagrams. The conclusion concerning secondary phase separation provided by slow diffusion in the percolation phase is supported by the following estimates. The characteristic diffusion time was estimated as $\tau_D \sim R^2/D$, where D is the constant of mutual diffusion. At the stage of coarsening, when the boundaries between the phases are well defined, for two phases, coefficients of mutual diffusion may be introduced: D for the matrix phase and D' for the percolation phase. At temperatures near the glass transition temperature T_g, D' is approximately 10^{-12} cm^2/s, and at temperatures far from T_g, D' is approximately 10^{-8} cm^2/s (A.E. Chalykh, private communication). In this case, for the highly viscous percolation phase, $\tau_{D'} \sim 10^6$ s (10 days), and for the low-viscous matrix phase $\tau_D \sim 100$ s. This value of $\tau_{D'}$ approximately corresponds to the time, when the coarsening percolation structure experiences secondary phase separation evidenced by the appearance of the PB-enriched droplets.

On the other hand, the time for shape relaxation induced by surface tension is controlled by hydrodynamic viscous flow within the percolation phase. This relaxation time may be estimated from the following relationship:

$$\tau_\sigma = R\eta'/k\sigma \ , \tag{6}$$

where $k = (\xi_o/2R)G(\eta'/\eta)$ and ξ_o is the amplitude of initial excitement [18]. For two-phase fluids with similar viscosities, k is approximately 0.04 [19–21]. In the case of two-phase fluids with quite different viscosities, at $R/\lambda_c \to 0$, when $\eta'/\eta \to \infty, G(\eta'/\eta) = 0$, whereas at $\eta'/\eta \to 0, G(\eta'/\eta) = 1$ [11]. In the case of an extremely high ratio between viscosities η'/η, assuming the invariability of $\xi_o/R = 0.5$ during hydrodynamic coarsening, one may estimate k to be about 0.15 (in the opposite case, $\eta'/\eta \to 0$, $k \approx 0.5$). When σ is about 0.1 dyne/cm (which is characteristic of partially compatible mixtures of polymers at temperatures about 15 K below T_g [22]), τ_σ is approximately 10^{12} s and η' is 10^{12} Pa s.

The values of τ_σ as well as the ratios $\tau_\sigma/\tau_{D'} \sim 10^6$ and $\tau_\sigma/\tau_D \sim 10^{10}$ are very high, and this evidence suggests that, at this stage, the rate of coarsening (the growth of domains) is controlled by very slow viscous flow ($\tau_\sigma \gg \tau_D$) within the percolation phase, and in the surrounding phase diffusion shows quasi-stationary character. These conditions provide rather fast attainment of a local concentration equilibrium at the phase boundaries, and the secondary phase separation is likely to be associated with slow diffusion within the percolation phase.

In some cases during the diffusion process the macromolecules cannot reach the boundary of the phase. It seems this is a common condition providing the secondary phase separation. It can be obtained in different ways: by a drastic decrease in the diffusion of the macromolecules as was observed in our experiments, and by fast hydrodynamic flow and coarsening of the phase with the nonequilibrium concentration so it takes much time to reach the border of the phase because of the large volume of the phase which means a long distance to be covered by the diffusing macromolecules. The last case was observed in the experiments of Tanaka [23]. According to Tanaka, the secondary phase separation is related to ''interface quenching'' provided by the fast (as compared with diffusion) hydrodynamic coarsening, which prevents the attainment of a local equilibrium at the phase boundary. Such a very fast formation of a large volume with nonequilibrium concentration became possible due to the wetting phenomenon: one of the components of the blend wets well the cover glasses and another component does not. So at the very beginning of the phase separation the glass-wetting phase flows in the direction of the glasses. In the experiments the secondary phase separation was studied only for critical mixtures. As spinodal decomposition took place, the whole wetting phase was a network and it could flow without macrodiffusion of the separated droplets or clusters, and the large volume of this phase with nonequilibrium concentration was formed near the cover glasses very quickly. The sample has a sandwich-like structure: top and bottom layers of one wetting phase near the cover glasses and the third layer of another phase in the middle. Both these phases were of nonequilibrium concentration.

Similar morphological structures were observed in experiments by Hasegawa et al. [24]. They discussed the pinning phenomenon which is considered as unique to the ordering process for an off-critical mixture with high molecular weight. This pinning phenomenon is proposed to originate from the dynamical percolation-to-cluster transition occurring during the coarsening process of the spinodal decomposition; however, there are some important differences. As was described earlier, in our experiments after a breakdown of the spinodal percolation structure network clusters were observed when close to the NPT. In the experiments of Hasegawa et al. the initial spinodal percolation breaks down into separated clusters of complicated form, but no real network clusters were registered. Another distinguishing difference is that we observed for the first time a new coarsening regime of the spinodal percolation at high supersaturations when the spinodal network contracts as a whole cluster to the center of the sample with subsequent secondary phase separation. The time scale of the phase separation in our case is much larger than that reported in Ref. [24].

Conclusions

Coupling between the phase separation and the glass transition provides a unique opportunity for a detailed characterization of morphological evolution in binary mixtures. In this work, for off-critical mixtures, changes in the regimes of evolution of nonequilibrium percolation structure near the NPT were described for the first time. At intermediate stages, this percolation structure either breaks down into individual ramified clusters (at low supersaturations) or experiences contraction to the center of the sample (at high supersaturations). In the latter case, within the coarsened structure, which exists in glassy state and is characterized by nonequilibrium concentration, secondary phase separation is observed.

Acknowledgement This work was supported by the Russian Fund for Fundamental Research (project no. 96-03-32523).

References

1. Cumming A, Wiltzius P, Bates FS (1990) Phys Rev Lett 65:863
2. Tomlins PE, Higgins JS (1989) J Chem Phys 90:6691
3. Nojima S, Ohyama Y, Yamaguchi M (1982) Polym J 14:907
4. Snyder HL, Meakin P, Reich S (1983) Macromolecules 16:757
5. Izumitani T, Takenaka M (1990) J Chem Phys 92:3213
6. Heermann DW, Binder K (1987) J Stat Phys 49:1053
7. Flory P (1953) Principles of polymer chemistry. Cornell University Press, Ithaca
8. Chan JW (1965) J Chem Phys 42:93
9. Langer JS, Baron M, Miller HD (1975) Phys Rev A 11:4

10. Radjabov TM (1990) Ph.D. thesis. Karpov Institute of Physical Chemistry, Moscow
11. Tomotika S (1935) Proc R Soc Lond A 150:322
12. Vinogradov GV, Malkin A Ya (1977) Rheology of polymers. Chemistry 30, Moscow
13. Berry GS, Fox TG (1968) Adv Polym Sci 5:261
14. Binder K (1994) Adv Polym Sci 112:181
15. Heermann DW (1984) Z Phys B 55:309
16. Heermann DW (1986) Phys Rep 136:153
17. Essam JW (1980) Rep Prog Phys 43:833
18. MacMaster LP (1975) Adv Chem Ser 142:43
19. San Miguel M (1985) Phys Rev A 31:1001
20. Guenoun P (1987) Phys Rev A 36:4876
21. Bates FS, Wiltzius P (1989) J Chem Phys 91:3258
22. Nose T (1995) Macromolecules 28:3702
23. Tanaka H (1994) Phys Rev Lett 72:3690
24. Hasegawa H, Shiwaku T, Nakai A, Hashimoto T (1998) In: Komura S, Furukawa H (eds) Dynamics of ordering process in condensed matter, N.Y. Plenum, p 457